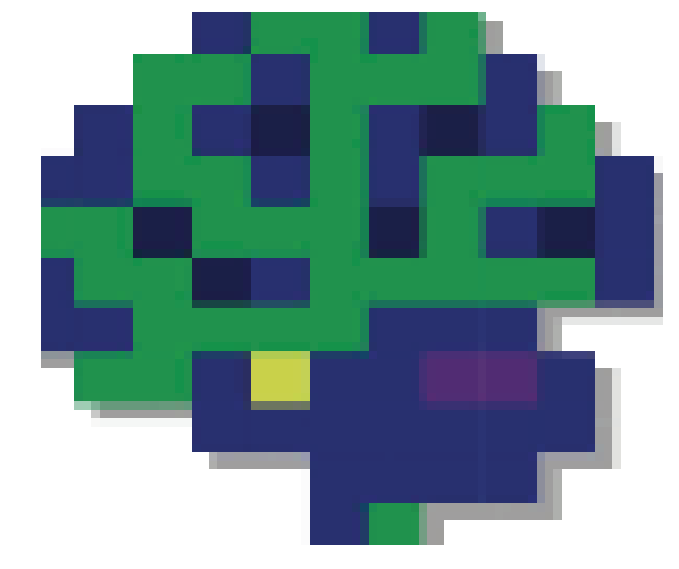


Effect of Context-Dependent Temporal Structure on Episodic Memory

S.H.P. Collin¹, R. Kempner², S. Srivatsan², A. Beukers², U. Hasson², K.A. Norman²

¹Tilburg University, Tilburg, Netherlands

²Princeton University, Princeton, USA



Introduction

Theories of schema-dependent memory posit that representing context-dependent temporal structure, such as the underlying schema, can boost memory for event details.

For example, these theories predict that, when we go to a restaurant, representing a restaurant schema can improve our memory for specific details during our time at the restaurant (e.g., Masís-Obando et al., 2022).

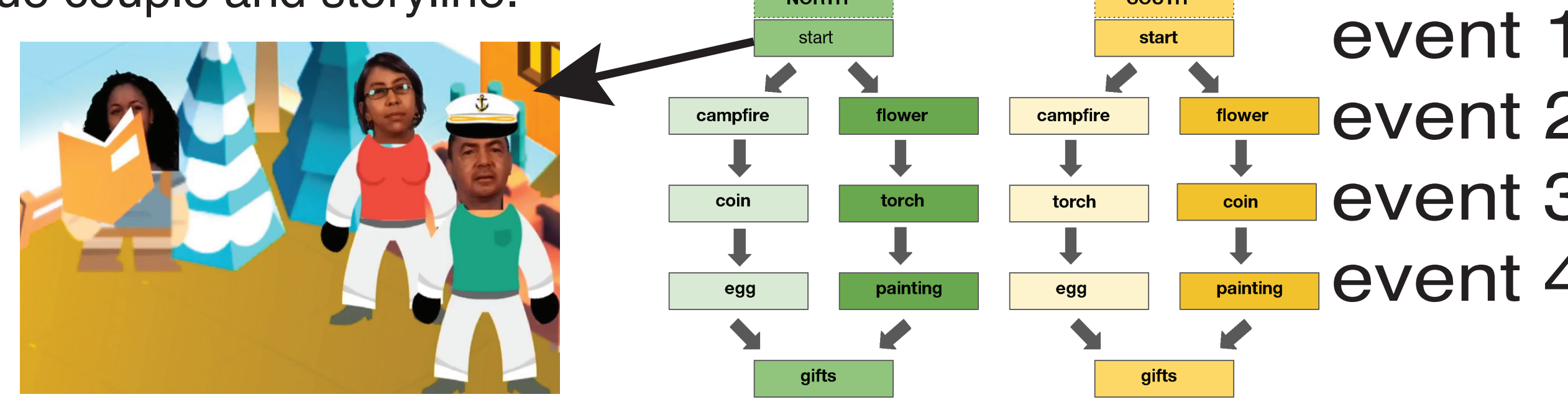
Restaurant schema



This study's goal is to investigate if and how memory performance relates to context-dependent temporal structure represented in the brain. The present work seeks to first uncover the neural representations of context-dependent temporal structure; in future work, we will relate those neural representations to memory performance.

Experimental Design

We ran a 2-day fMRI study ($N = 40$) in which we exposed participants to animated videos of wedding ceremonies. The wedding videos consist of sequences of ritual events drawn from one of the four paths in the north or south schema. Each wedding video has a unique couple and storyline.

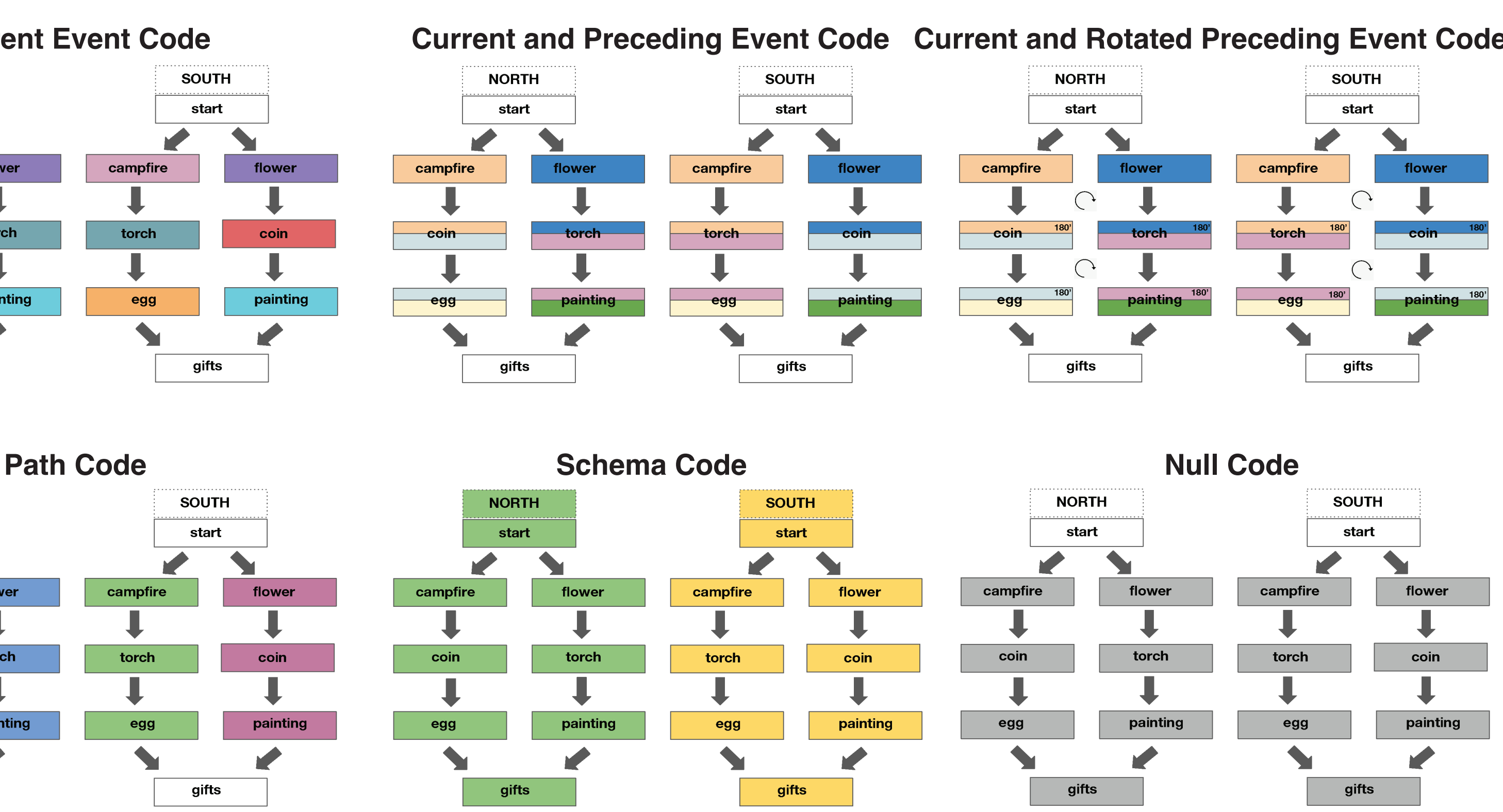


On Day 1, participants learned the structure of the wedding ritual sequences by viewing many wedding ceremonies and answering questions about them. On Day 2, in the fMRI scanner, they watched and then recalled 12 new wedding ceremony videos.

Analysis Plan

How can we uncover the neural representations of context-dependent temporal structure when participants watched the 12 wedding ceremony videos on Day 2 in the fMRI scanner?

First, consider the following examples of possible context-dependent and non-context-dependent codes that might be represented in the brain:



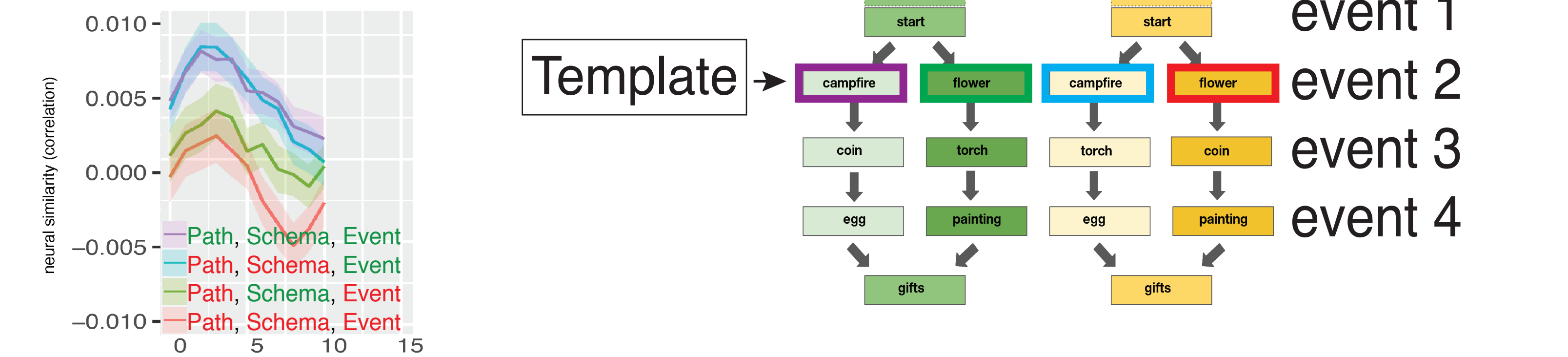
Since these neural codes make specific predictions about which events will have more or less similar neural activity, running a representational similarity analysis (RSA) comparing each event to all other events would allow us to search for these codes as well as other possible codes.

First, we ran the RSA on each searchlight (i.e. a sphere of voxels in the fMRI recordings). Then, we clustered searchlights by their RSA results using Kmeans to uncover the brain regions where possible codes may be represented. Next, we evaluated the results to investigate whether the clusters contained codes.

RSA Procedure

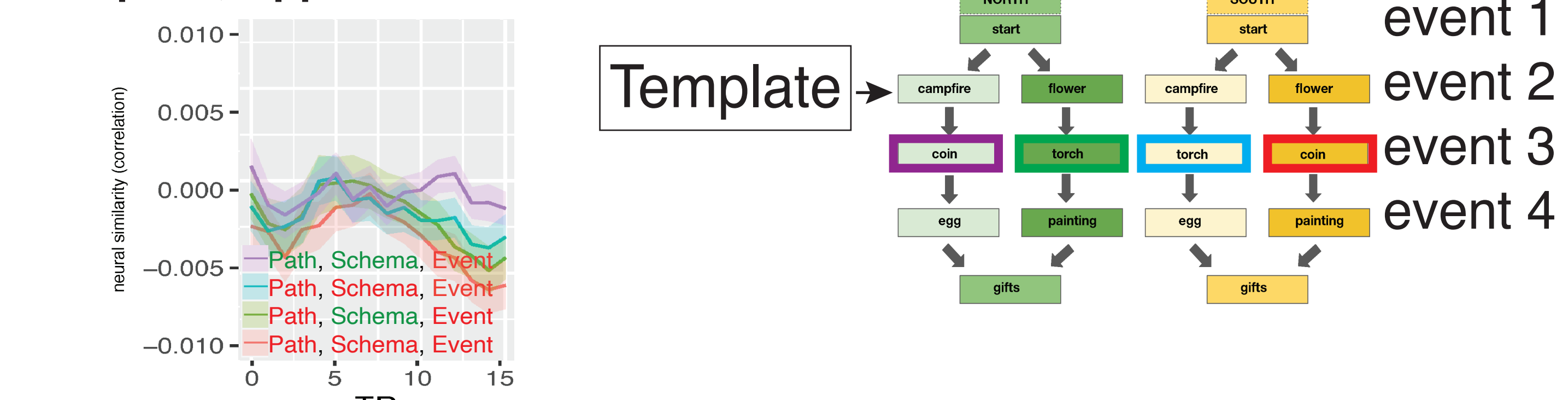
Get the average neural activity during one event on the event 2 level as the “template” and correlate with neural activity at each TR from all events at the event 2 level in all weddings.

Event 2 Template, Applied to TRs in Event 2



We can also correlate a template on the event 2 level with events on the 3 or 4 level.

Event 2 Template, Applied to TRs in Event 3



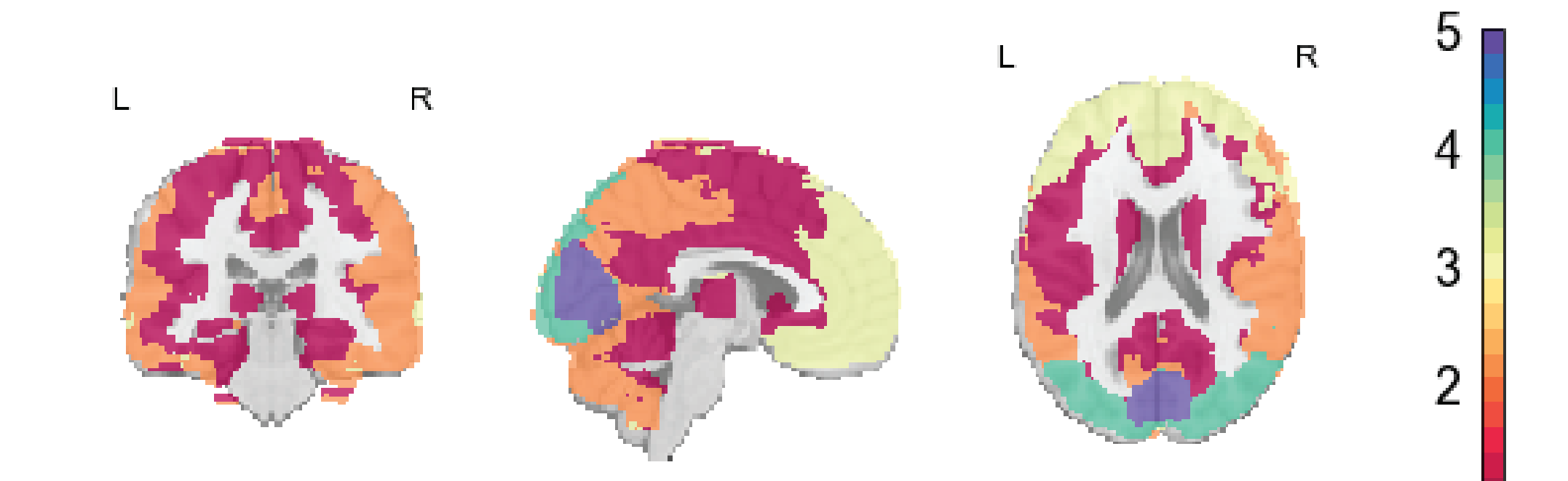
Correlating each event level with each other level, we get a 3 by 3 RSA matrix.

Results

After investigating Kmeans results from $K = 2$ to $K = 7$, we found that $K = 5$ yielded a solution where all of the clusters were interpretable and distinct.

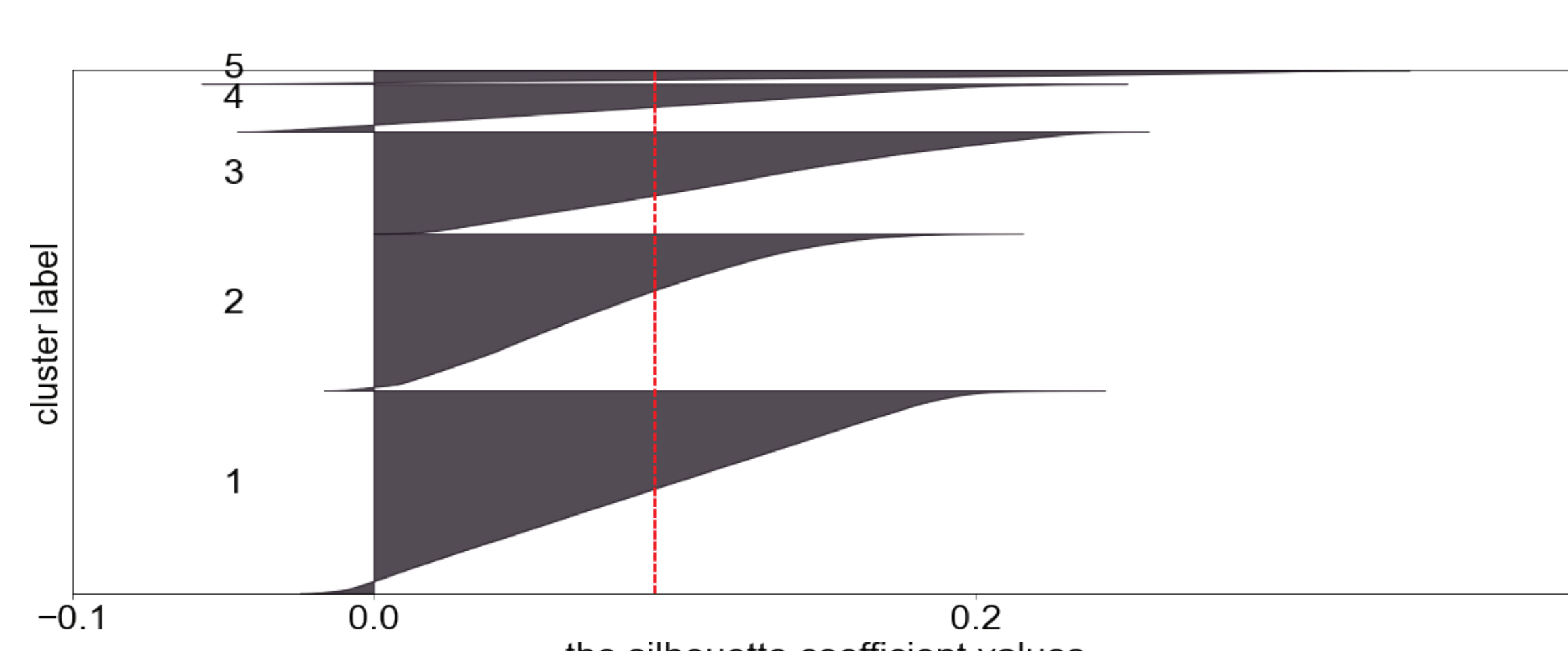
The silhouette scores and anatomical distributions were also reasonable with $K = 5$. Cluster 3 was a null cluster with no significant differences between the events.

Brain Map of Clusters Found by Kmeans with $K = 5$



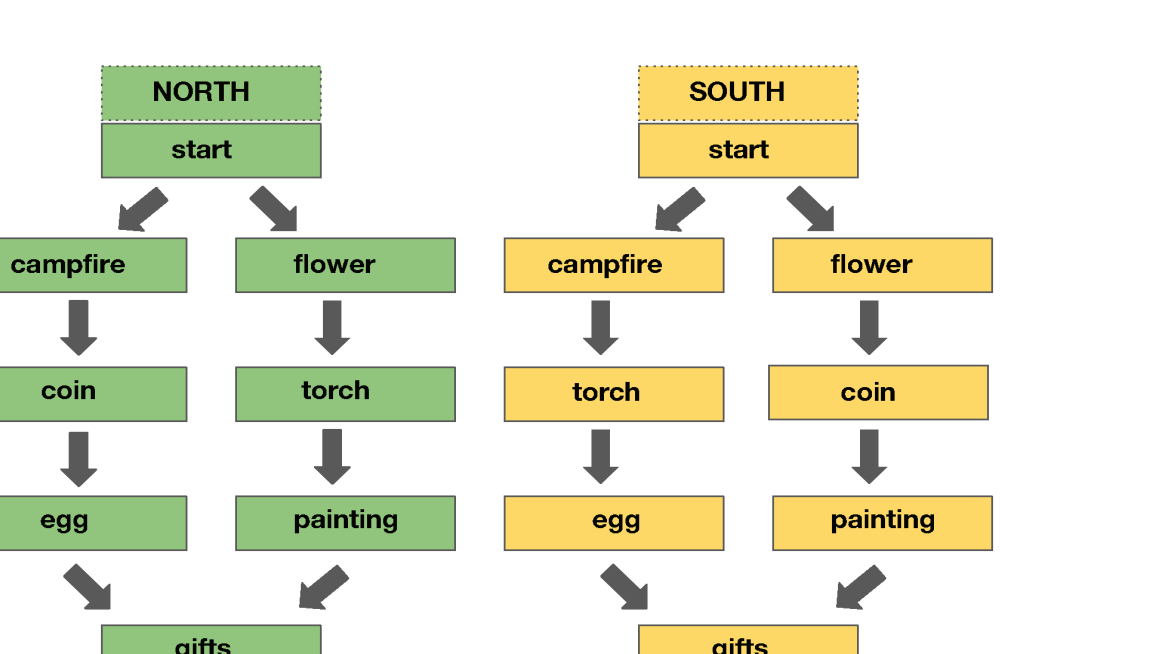
Schema code is cluster 1 (red). Path code is cluster 2 (orange). Null code is cluster 3 (yellow). Event code is cluster 4 (turquoise). Current and rotated preceding event code is cluster 5 (purple).

Silhouette Scores with $K = 5$



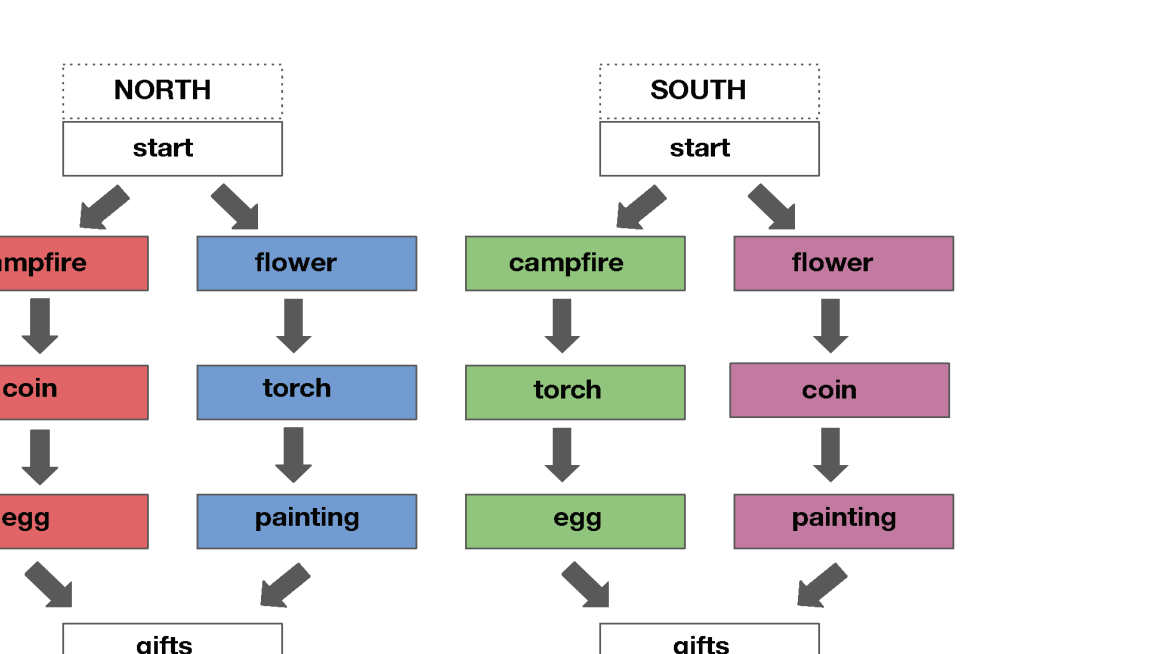
Silhouette scores measure how close data points are to their assigned cluster and how far away data points are to other clusters (the higher the score, the better). The small number of negative data points indicates that most of the searchlights were well-clustered with $K = 5$.

Cluster 1 (Schema Code)



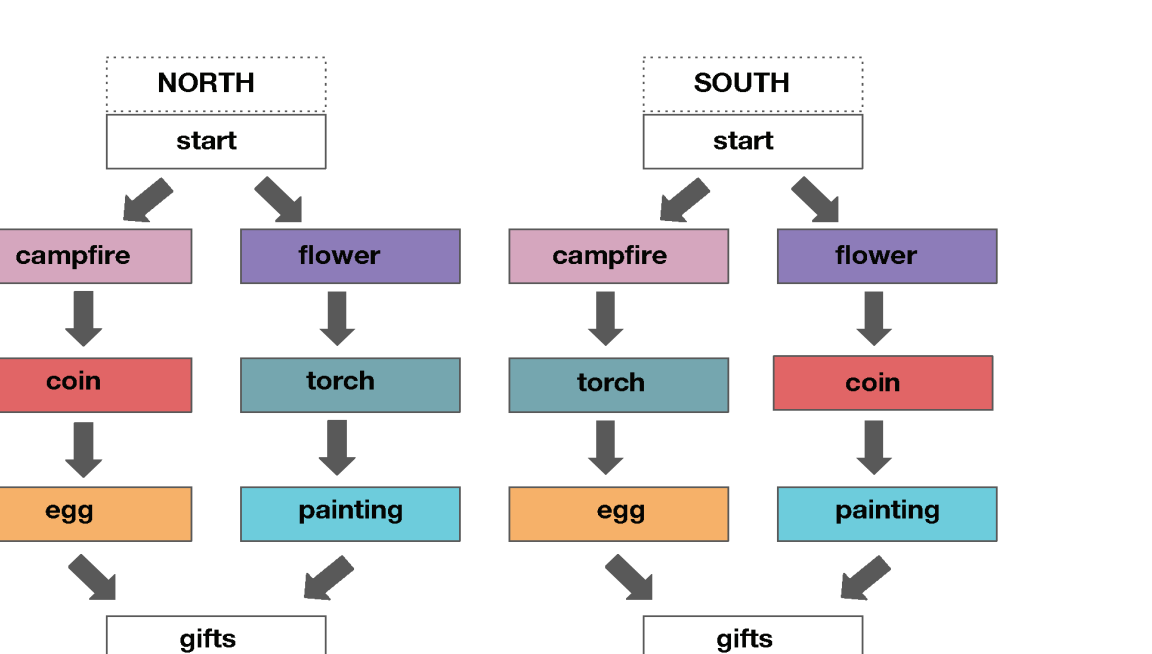
This region codes for the schema so neural activity is similar when the schemas are the same.

Cluster 2 (Path Code)



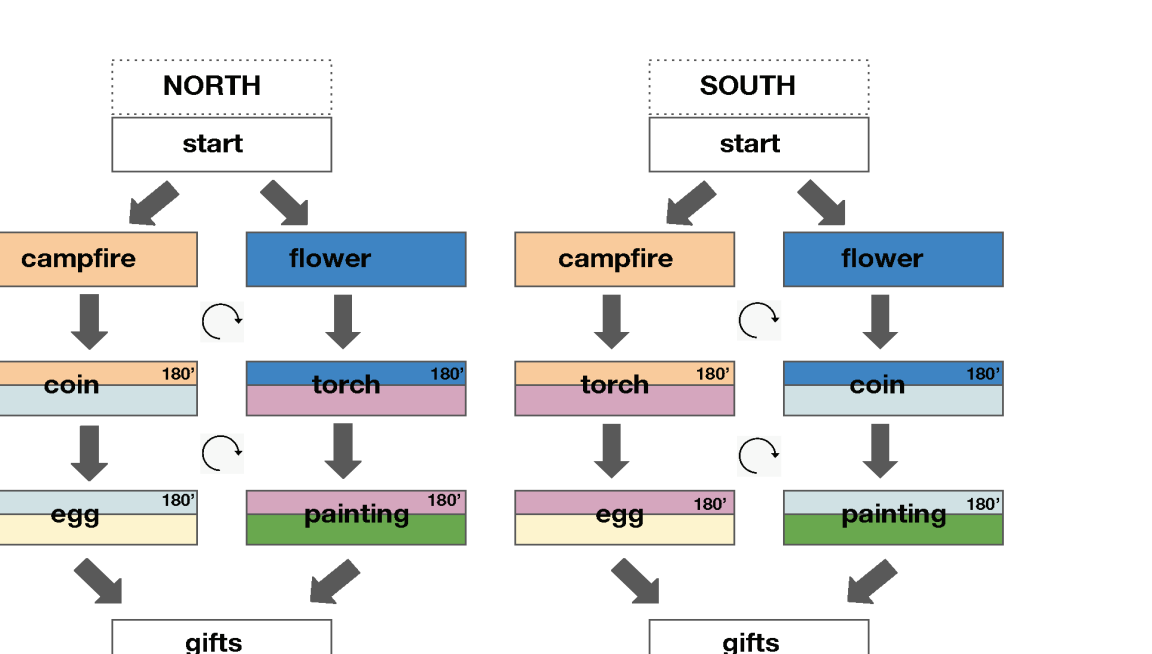
This region codes for the path so neural activity is similar when the paths are the same.

Cluster 4 (Event Code)



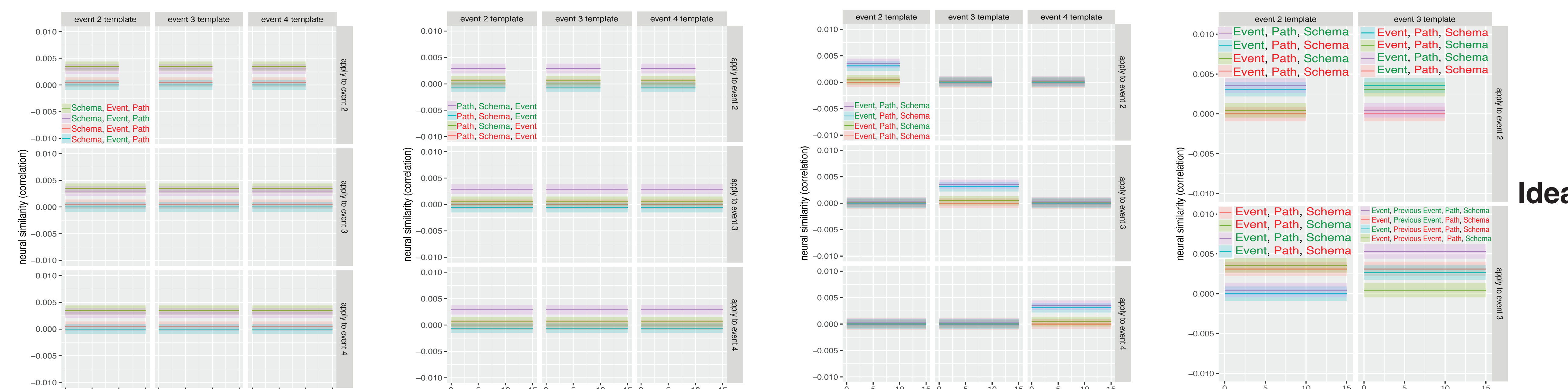
This region codes for the current event so neural activity is similar when the events are the same.

Cluster 5 (Rotated Code)

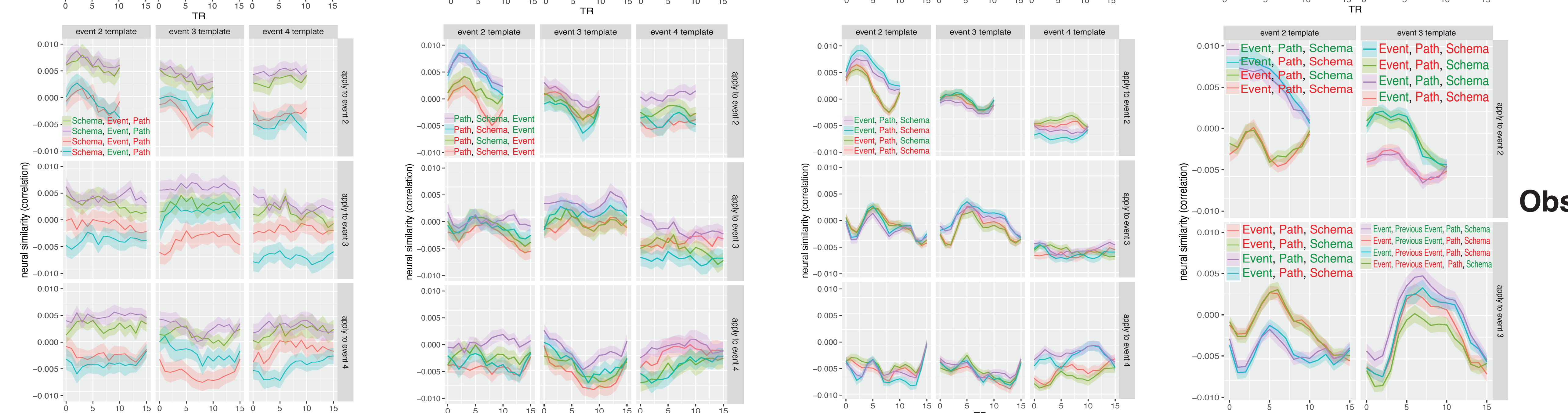


This region codes for both the current and rotated preceding event.

Ideal



Observed



Conclusions

Different temporal structure codes make specific predictions about which events will have more or less similar neural activity. Therefore, we used RSA on fMRI data during wedding ceremony viewing to search the brain for codes.

By clustering the searchlights' RSA results using Kmeans, we found four qualitatively distinct codes that were represented in the brain during wedding ceremony viewing: event code, current and rotated preceding event code, schema code, and path code.

The presence of rotated preceding event codes fits with other recent work by Libby & Buschman (2021), Wan et al. (2020), and van Loon et al. (2018).

Now that we have a better understanding of what temporal structure codes exist in the brain during wedding viewing, and where they are anatomically, we can relate those neural representations to memory performance during recall.

References

- Libby, A., & Buschman, T. J. (2021). Rotational dynamics reduce interference between sensory and memory representations. *Nature neuroscience*, 24(5), 715-726.
- Masís-Obando, R., Norman, K. A., & Baldassano, C. (2022). Schema representations in distinct brain networks support narrative memory during encoding and retrieval. *Elife*, 11, e70445.
- van Loon, A. M., Olmos-Solis, K., Fahrenfort, J. J., & Olivers, C. N. (2018). Current and future goals are represented in opposite patterns in object-selective cortex. *Elife*, 7, e38677.
- Wan, Q., Cai, Y., Samaha, J., & Postle, B. R. (2020). Tracking stimulus representation across a 2-back visual working memory task. *Royal Society open science*, 7(8), 190228.
- This work was supported by ONR MURI grant N00014-17-1-2961 to KAN and UH